BIOCHEMISTRY
including biophysical chemistry & molecular biology
Article

Biochemistry **2010,** *49,* 3191–3202 3191
DOI: 10.1021/bi100104e

Role of Lipid Peroxidation in Cellular Responses to D,L-Sulforaphane, a Promising Cancer Chemopreventive Agent†

Rajendra Sharma,*,‡ Abha Sharma,‡ Pankaj Chaudhary,‡ Virginia Pearce,§ Rit Vatsyayan,‡ Shivendra V. Singh,∥ Sanjay Awasthi,‡ and Yogesh C. Awasthi‡

‡*Department of Molecular Biology and Immunology, University of North Texas Health Science Center, Fort Worth, Texas 76107,* §*Department of Pharmacology and Neuroscience, University of North Texas Health Science Center, Fort Worth, Texas 76107, and* ∥*Department of Pharmacology and Chemical Biology, University of Pittsburgh, Pittsburgh, Pennsylvania 15260*

Received January 22, 2010; Revised Manuscript Received March 4, 2010

ABSTRACT: D,L-Sulforaphane (SFN), a synthetic analogue of the broccoli-derived L-isomer, is a highly promising cancer chemopreventive agent substantiated by inhibition of chemically induced cancer in rodents and prevention of cancer development and distant site metastasis in transgenic mouse models of cancer. SFN is also known to inhibit growth of human cancer cells in association with cell cycle arrest and reactive oxygen species-dependent apoptosis, but the mechanism of these cellular responses to SFN exposure is not fully understood. Because 4-hydroxynonenal (4-HNE), a product of lipid peroxidation (LPO), the formation of which is regulated by hGSTA1-1, assumes a pivotal role in oxidative stress-induced signal transduction, we investigated its contribution in growth arrest and apoptosis induction by SFN using HL60 and K562 human leukemic cell lines as a model. The SFN-induced formation of 4-HNE was suppressed in hGSTA1-1-overexpressing cells, which also acquired resistance to SFN-induced cytotoxicity, cell cycle arrest, and apoptosis. While resistance to SFN-induced cell cycle arrest by ectopic expression of hGSTA1-1 was associated with changes in levels of G2/M regulatory proteins, resistance to apoptosis correlated with an increased Bcl-xL/Bax ratio, inhibition of nuclear translocation of AIF, and attenuated cytochrome *c* release in cytosol. The hGSTA1-1-overexpressing cells exhibited enhanced cytoplasmic export of Daxx, nuclear accumulation of transcription factors Nrf2 and HSF1, and upregulation of their respective client proteins, γ-GCS and HSP70. These findings not only reveal a central role of 4-HNE in cellular responses to SFN but also reaffirm that 4-HNE contributes to oxidative stress-mediated signaling.

D,L-Sulforaphane (SFN),[1] a synthetic analogue of the naturally occurring L-isomer abundant in several cruciferous vegetables (e.g., broccoli), is a potent inhibitor of chemically induced cancer in experimental rodents (*1*−*5*). It has been shown to modulate inflammation, induce apoptosis, cause cell cycle arrest, and inhibit several phase 1 enzymes that may activate chemical carcinogens (*1*). Even though the mechanisms of the chemopreventive activities of SFN are not completely understood, it has been suggested that besides inhibiting phase I enzymes, SFN can also induce phase 2 detoxification enzymes such as glutathione transferases (GSTs) through transcriptional activation of antioxidant response element (ARE)-driven genes regulated by nuclear factor E2-related factor-2 or Nrf2 (*1*, *6*−*8*). Being an electrophile, SFN causes oxidative stress by generating reactive oxygen species (ROS) that are believed to contribute to its biological properties (*1*). ROS-mediated signaling for cell cycle arrest and apoptosis along with DNA damage and depleted cellular glutathione (GSH) levels are also implicated in the mechanisms of its chemopreventive activity (*1*−*8*).

Membrane lipid peroxidation (LPO) is an inevitable consequence of ROS-induced oxidative stress, and there is ample evidence that the electrophilic LPO products, including lipid hydroperoxides and α,β-unsaturated carbonyls, particularly 4-hydroxynonenal (4-HNE), play a crucial role in ROS-induced signaling (*9*−*13*). In recent years, 4-HNE has emerged as an important second-messenger molecule involved in signaling for cell proliferation, cell cycle arrest, differentiation, apoptosis, and regulation of the expression of a multitude of genes in cells of diverse origin (*9*−*17*). 4-HNE has also been shown to modulate survival and death signaling pathways in a concentration-dependent manner by interacting with several signaling proteins involved in both the extrinsic and the intrinsic pathways of apoptosis (*18*, *19*). Furthermore, 4-HNE has been shown to modulate the expression and functions of stress-responsive transcription factors, Nrf2 (*20*) and heat shock factor1 (HSF1), and the transcription repressor, Daxx or death-associated Fas interacting protein (*19*, *21*, *22*).

Because ROS are implicated in the biological activities of SFN, we reasoned that ROS-induced LPO products, particularly 4-HNE, could contribute to these activities. We have tested this

†Supported in part by National Institutes of Health Grants ES012171, EY04396 (Y.C.A.), CA77495 (S.A., and supplement to this grant to A. S.), and CA115498 (S.V.S.).

*To whom correspondence should be addressed: Department of Molecular Biology and Immunology, University of North Texas Health Science Center, Fort Worth, TX 76107. Telephone: (817) 735-2140. Fax: (817) 735-2118. E-mail: rsharma@hsc.unt.edu.

[1]Abbreviations: SFN, D,L-sulforaphane; 4-HNE, 4-hydroxynonenal; GST, glutathione transferase; hGSTA1-1, human glutathione transferase isozyme A1-1; LPO, lipid peroxidation; ROS, reactive oxygen species; GSH, glutathione; Daxx, death-associated Fas binding protein; Nrf2, nuclear factor E2-related factor 2; HSF1, heat shock factor 1; CDNB, 1-chloro-2.4-dinitrobenzene; FACS, fluorescence-activated cell sorting.

Published on Web 03/05/2010

postulate by studying the effects of SFN in an in vitro model in which ROS-induced LPO has been suppressed by overexpression of the α class GSTA1-1 isozyme. Apart from catalyzing the conjugation of toxic electrophiles to GSH, GST A1-1 also catalyzes the GSH-dependent reduction of phospholipid hydroperoxides (PL-OOH) and fatty acid hydroperoxides (FA-OOH) through its Se-independent glutathione peroxidase (GPx) activity, thereby terminating the autocatalytic chain of LPO reactions resulting in decreased intracellular 4-HNE levels (*14*, *15*, *23*). Previous studies conducted on various GSTA1-1-transfected cell types in culture have shown that these cells have reduced 4-HNE levels and acquire resistance to ROS-induced apoptosis (*9*, *17*, *23*). Our studies were designed to elucidate the putative contributions of 4-HNE in the mechanisms of SFN-induced cytotoxicity and signaling in two human leukemic cell lines, viz., HL60, derived from a promyelocytic leukemia patient, and K562, which originated from chronic myelogenous leukemia having specific chromosome abnormality designated as Philadelphia chromosome (*24*). Specifically, we have addressed the question of whether the overexpression of hGSTA1-1 can affect SFN-induced cytotoxicity and signaling events by modulating intracellular levels of 4-HNE in these cells. We have also studied the effects of SFN on cell cycle arrest and apoptosis-related proteins, stress-responsive transcription factors Nrf2, HSF1, and transcription repressor Daxx. Furthermore, we have examined whether these effects of SFN can be abrogated by the overexpression of GSTA1-1 in these cells. Results of these studies strongly indicate that 4-HNE plays a crucial role in the mechanisms of SFN-induced signaling. Our data also suggest that the α-class GSTs can modulate cell survival and death signaling by regulating the intracellular concentrations of 4-HNE which reinforces our previous assertion that these enzymes play an important role in the overall regulation of ROS-induced signaling.

MATERIALS AND METHODS

Materials. Epoxy-activated Sepharose 6B, glutathione (GSH), 1-chloro-2,4-dinitrobenzene (CDNB), cumene hydroperoxide (CU-OOH), and 3-(4,5-dimethylthiazol-2-yl)-2,5-diphenyltetrazolium bromide (MTT) were obtained from Sigma (St. Louis, MO). RPMI 1640 medium, fetal bovine serum, phosphate-buffered saline (PBS), and penicillin/streptomycin were purchased from GIBCO, Inc. (Grand Island, NY). All reagents for sodium dodecyl sulfate−polyacrylamide gel electrophoresis (SDS−PAGE) and Western transfer were purchased from Invitrogen (Carlsbad, CA). Sulforaphane (SFN) was obtained from Sigma.

Antibodies. Antibodies against Bax (N-20, sc-493, polyclonal), caspase-3 (sc-7148, polyclonal), Bcl-xL (sc-23958, monoclonal), Nrf2 (sc-722, polyclonal), Daxx (sc-7152, polyclonal), and HSF1 (sc-9144, polyclonal), Hsp 70, cyclin B1 (sc-595), cdk1/cdk2 (sc-53219), histone 3 (sc-H0164, polyclonal), and VDAC1 (sc-8829, polyclonal) were obtained from Santa Cruz Biotechnology (Santa Cruz, CA), while AIF (4642, polyclonal) was obtained from Cell Signaling Technology, Inc. Horseradish peroxidase (HRP)-conjugated secondary antibodies as well those against GAPDH were purchased from Southern Biotech (Birmingham, AL). Polyclonal antibodies raised against the human α-class GSTs and the GPx were the same as those used in our previous studies (*15*). Antibodies against the 4-HNE−protein adduct (4-HNE 11S) were purchased from Alpha Diagnostics (San Antonio, TX).

Cell Cultures. HL60 and K562 cells were grown as suspension cultures in RPMI 1640 medium containing L-glutamine supplemented with 10% (v/v) fetal bovine serum and 1% penicillin/streptomycin (v/v) at 37 °C in a 5% CO_2 humidified atmosphere. Cells were passaged by mechanical desegregation and transfer of a small number of cells to new flasks.

Stable Transfection with hGSTA1. On the basis of the previously reported cDNA sequence for *hGSTA1* (*23*), PCR primers were designed to amplify the complete coding sequence (656 bp) of *hGSTA1* from the pET-30a (+)/*hGSTA1* vector. The amplified cDNA was subcloned into the pTarget-T mammalian expression vector (Promega). Cells were then transfected with pTarget-T/*hGSTA1*, or with the vector alone, using the Lipofectamine Plus reagent (Invitrogen, San Diego, CA) according to the manufacturer's instructions. Stable transfectants were isolated by selection on 300 μg/mL G418 for ∼2 weeks. Single clones of stably transfected cells were obtained by limiting dilution. Further characterization of the selected G418-resistant stable clones expressing hGSTA1-1 was achieved by Western blotting and enzyme assays.

Enzyme Assays. For the determination of the activity of the antioxidant enzymes and the enzymes involved in GSH homeostasis in the pTarget-T/*hGSTA1*- or empty vector-transfected cells, the respective cells were homogenized in buffer A containing 1.4 mM β-mercaptoethanol (β-Me) by sonication. The sonicated cells were centrifuged for 45 min at 28000*g* and 4 °C, and the 28000*g* supernatant was then subjected to GSH affinity chromatography (*25*). Purified hGSTA1-1 was eluted from the GSH affinity resin in 50 mM Tris-HCl (pH 9.6) containing 10 mM GSH and 1.4 mM β-Me. Enzyme activities were assayed both in the crude 28000*g* fraction and in purified hGSTA1-1.

GST activity toward CDNB (*26*) and SFN (*27*), GPx activity toward cumene hydroperoxide (CU-OOH) (*28*), and the activities of glutathione reductase (GR) and γ-glutamylcysteine synthetase (γ-GCS) were determined by the previously reported methods (*29*, *30*).

Western Blot Analysis. For the detection of the expressed hGSTA1-1 protein, stably transfected HL60 and K562 cells were collected by centrifugation for 5 min at 500*g*, washed twice with PBS, and resuspended in hypotonic lysis buffer (buffer A). After a brief sonication for 15 s, three times each, the cell lysate was centrifuged at 28000*g* and the supernatants were measured for protein concentration by the Bradford method (*31*). Cell lysates containing 50 μg of protein were separated with 12% polyacrylamide gels according to the method of Laemmli (*32*) and subjected to Western blot analysis essentially according to the method of Towbin et al. (*33*) using the polyclonal antibodies against the human α-class GSTs. Chemiluminescence reagents (Invitrogen) were used to develop the immunoblots by following the manufacturer's instructions.

For detection of other proteins, treated cells were collected, washed with PBS, and resuspended in radio-immunoprecipitation assay (RIPA) lysis buffer, containing 1× PBS, (pH 7.4), 1% Nonidet P-40 (NP-40), 0.5% sodium deoxycholate, 0.1% sodium dodecyl sulfate, 1 mM phenylmethanesulfonyl fluoride (PMSF), and 2 μg/mL pepstatin. After being sonicated three times for 5 s, the lysates were centrifuged at 14000 rpm for 15 min and the supernatants collected. Subcellular fractionated extracts containing cytoplasmic, mitochondrial, and nuclear proteins were prepared by a modification of the published procedure used previously (*34*). Protein concentrations in various extracts were determined by the Bradford assay (*31*). Separation of proteins in

the various extracts was ascertained by Western blot analysis using marker antibodies for different proteins as described above.

Cytotoxicity Assays. The sensitivity of the cells to SFN was measured by the MTT assay as described by Mosmann (*35*) with slight modifications. Briefly, 2×10^4 cells in 190 μL of medium were plated on each well in 96-well flat-bottom microtiter plates; 10 μL of PBS containing various amounts of SFN was added. Eight replicate wells for each concentration of SFN were used in these experiments. Following incubation of the plates at 37 °C for 24 h, 10 μL of MTT solution (5 mg/mL in PBS) was added to each well, and the plates were incubated for an additional 4 h at 37 °C. The plates were centrifuged at 2000*g* for 10 min. The medium within the wells was aspirated, and 100 μL of dimethyl sulfoxide (DMSO) was added to each well. The intracellular formazan dye crystals were dissolved when the plates were shaken at room temperature for 2 h. The absorbance of formazan at 562 nm was measured using a microplate reader (Elx808 BioTek Instruments, Inc.). The concentration of SFN resulting in a 50% decrease in the level of formazan formation (IC_{50}) was obtained by plotting a dose−response curve.

Determination of Cellular GSH Levels. The intracellular GSH content was determined in cellular homogenates prepared in buffer A without β-mercaptoethanol by the method of Beutler et al. (*36*). Briefly, cells were resuspended in buffer A and sonicated. To 200 μL of the lysate was added 300 μL of precipitating solution (0.2 M glacial *m*-phosphoric acid, 5 M NaCl, and 5 mM EDTA). The acid-precipitated proteins were pelleted by centrifugation at 4 °C for 10 min at 20000*g*. To determine the GSH content, 200 μL of the acid-soluble supernatants was mixed with 800 μL of 0.3 M Na_2HPO_4 and mixed, and the initial OD was read at 412 nm; 100 μL of 0.6 mM 5,5-dithiobis(2-nitrobenzoic acid) (DTNB in 1% sodium citrate) was added to a final volume of 1 mL. The increase in absorption at 412 nm was monitored and used to determine the amount of GSH in the samples.

Determination of the Intracellular 4-HNE Levels. Intracellular levels of 4-HNE in the control and 20 μM SFN-treated cells (2×10^7) were determined spectrophotometrically by using the LPO 586 (Oxis International) measurement kit per the manufacturer's instructions.

Immunofluorescence Detection of 4-HNE−Protein Adducts and Localization of Nrf2. Control and SFN-treated HL60 cells were washed twice with ice-cold phosphate-buffered saline (PBS) (pH 7.4). These cells were spread onto clean glass slides, using a cytospin (Cytospin 2), fixed with 4% paraformaldehyde for 30 min at room temperature, and permeabilized with 0.1% Triton X-100 for 30 min. Slides were once again washed with PBS and blocked with 3% goat serum in PBS for 2 h. For the immunofluorescence detection of 4-HNE adducts, cells were incubated with primary antibodies (1:250) against the 4-HNE−protein adduct overnight at 4 °C in a humidified chamber. After being washed for 3×10 min with PBS, cells were incubated with TRITC-conjugated anti-mouse secondary antibodies (1:1000) for 2 h. Slides were mounted in a medium containing 1.5 μg/mL DAPI (Vector Laboratories, Inc.) and observed under the fluorescence microscope (Olympus, Tokyo, Japan). For the immunofluorescence detection of Nrf2, control and SFN-treated cells were processed in a similar manner as described above except that these cells were incubated with anti-Nrf2 antibody diluted 1:50 in PBS containing 1% bovine serum albumin overnight at 4 °C. After being washed with ice-cold PBS, the slides were incubated with FITC-labeled goat anti-rabbit immunoglobulin G (1:100) (Southern Biotech) for 2 h at room temperature. The slides were viewed under a Nikon E600 microscope with a 40× objective using filters for DAPI, FITC, and TRITC stains.

Flow Cytometric Analysis. The effect of SFN on cell cycle distribution was determined by FACS analysis according to the protocol provided by the Flow Cytometry & Laser Capture Microdissection Core Facility, University of North Texas Health Science Center. Cells (2×10^5 in a 100 mm dish) were treated with 20 μM SFN for 5 and 24 h at 37 °C. Appropriate controls were also set up. Care was taken to ensure that the cells were no more than 50% confluent on the day of the treatment. After being treated, floating and adherent cells were collected, washed with PBS two times by centrifugation at 300*g* for 5 min at 4 °C, and fixed with 70% ethanol. On the day of flow analysis, cell suspensions were centrifuged and counted, and approximately 600000 cells were resuspended in 500 μL of PBS in flow cytometry tubes. Cells were treated with 2.5 μL of RNase (20 mg/mL) and incubated at 37 °C for 30 min, after which they were treated with 5 μL of a propidium iodide (1 mg/mL) solution and incubated at room temperature for 30 min in the dark. The stained cells were analyzed using the Beckman Coulter Cytomics FC500, Flow Cytometry Analyzer. CXP2.2 analysis software from Beckman Coulter was used to deconvolute the cellular DNA content histograms to quantitate the percentage of cells in the respective phases (G1, S, and G2/M) of the cell cycle. The appearance of the sub-G0/G1 peak indicates cells undergoing apoptosis.

Statistical Analysis. Data presented are means ± the standard deviation (SD) of triplicate samples from three different experiments. Statistical significance between different groups was determined using a Student's *t* test. A p value of < 0.05 was considered significant.

RESULTS

Stable Transfection of hGSTA1 in HL60 and K562 Cells. The cells were separately transfected with pTarget empty vector, and the pTarget-T/*hGSTA1* cDNA. Subsequent selection of stably transfected clones in the presence of G418 resulted in a high level of expression of hGSTA1-1 as indicated by the results of Western blot analysis shown in panels A and B of Figure 1, where the *hGSTA1*-transfected cells showed a robust expression of hGSTA1-1 while the wild-type and empty vector-transfected cells did not show any detectable expression of hGSTA1-1. There were no noticeable differences in the morphology or growth kinetics of the empty vector and *hGSTA1*-transfected cells.

GST activity toward 1-chloro-2,4-dinitrobenzene (CDNB) was found to be increased by almost 2-fold in *hGSTA1*-transfected cells, whereas selenium-independent GPx activities toward cumene hydroperoxide (CU-OOH) in *hGSTA1*-transfected cells was increased ~4.5-fold as compared to that in empty vector-transfected cells. Smaller increases in the conjugating activity against CDNB is perhaps caused by the high constitutive level of this activity in cells (Table 1). Together, these results confirmed the presence of a functional hGSTA1-1 protein in the transfected cells. Similar to that observed in our previous studies (*16*, *17*), the activities of catalase, superoxide dismutase, and GPx activity toward H_2O_2 were comparable in the vector- and *GSTA1*-transfected cells. Since GSTA1-1 has no GPx activity toward H_2O_2, these results indicated that the capacities of the empty vector or the *GSTA1*-transfected cells to detoxify H_2O_2 and superoxide were similar. There was a 2-fold increase in the

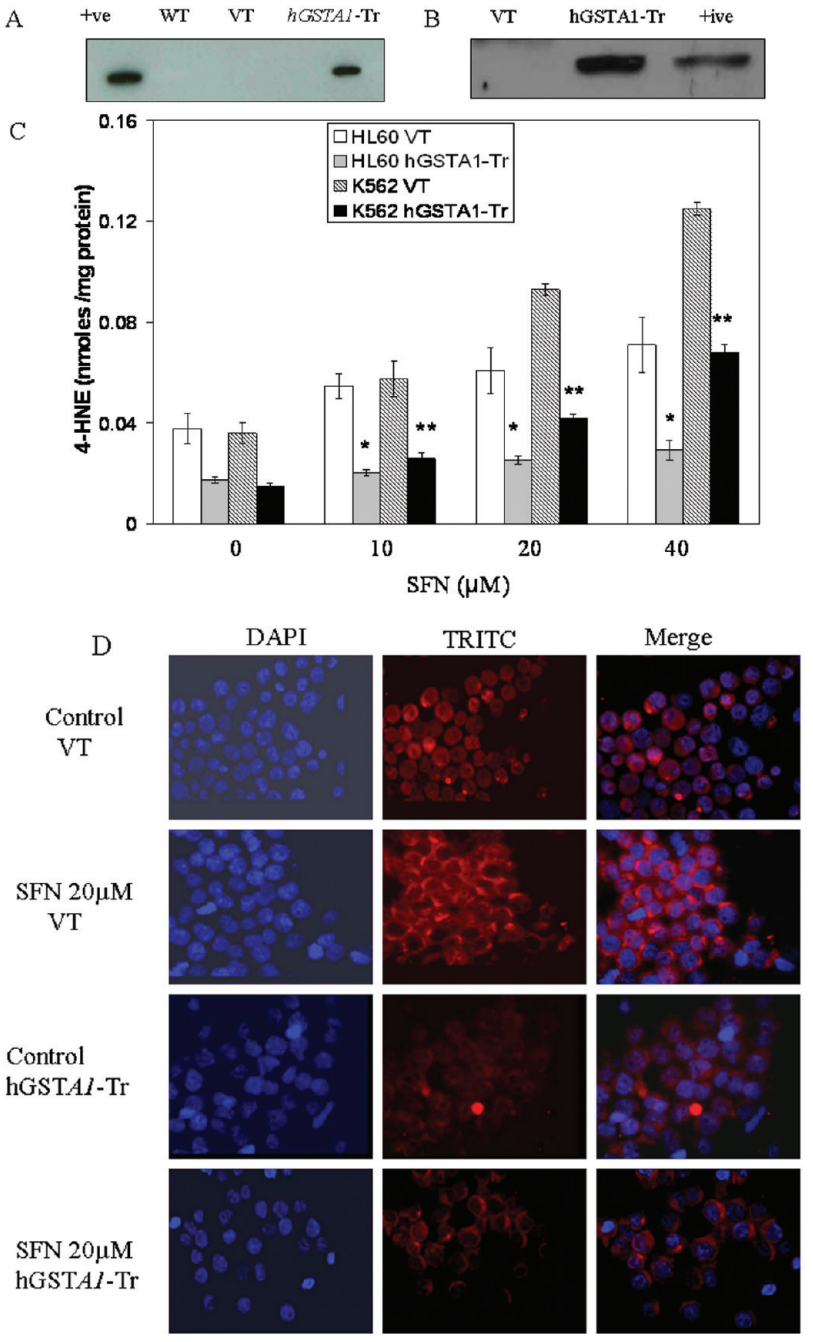

FIGURE 1: Expression of hGSTA1-1 in *hGSTA1*-transfected cells. HL60 (A) and K562 (B) cells were transfected with the cDNA of *hGSTA1* cloned in the pTarget-T mammalian expression vector or the vector alone as described in Materials and Methods. The supernatant fraction (28000*g*) of homogenates of the wild-type (WT), vector (VT), and *hGSTA1*-transfected (*hGSTA1-Tr*) HL60 cells containing 30 μg of protein was subjected to SDS−PAGE in a 12% gel. Expression of hGSTA1-1 in the stably transfected clone selected in G418 (300 μg/mL) was analyzed by Western blot analysis using polyclonal primary antibodies against human α-class GSTs raised in rabbits and peroxidase-conjugated goat anti-rabbit secondary antibodies. The blot was developed using chemiluminescence (Supersignal West Pico, Pierce) reagents. Lanes have been appropriately marked on the immunoblots. A representative immunoblot from one of the several hGSTA1-1-expressing clones selected is shown. (C) Levels of 4-HNE in SFN-treated vector- and hGSTA1-1-expressing HL60 and K562 cells. Vector- and hGSTA1-1-expressing cells (2×10^7) were incubated with RPMI complete medium containing SFN (0−40 μM) for 5 h at 37 °C. After being pelleted by centrifugation, cells were washed and sonicated (3×10 s at 30 W) in PBS containing BHT (final concentration of 5 mM) on ice. 4-HNE levels in the cell pellets were measured by using the LPO-586 kit per the manufacturer's instructions. Data presented are means ± SD [$n = 3$; one asterisk and two asterisks denote significant differences in 4-HNE levels of vector- and hGSTA1-1-expressing HL60 and K562 cells, respectively ($p < 0.05$)]. (D) Immunofluorescence analysis of 4-HNE adducts in SFN-treated vector- and hGSTA1-1-expressing HL60 cells. Vector- and hGSTA1-1-expressing HL60 cells (1×10^6) were treated with SFN (20 μM) for 2 h at 37 °C in RPMI complete medium. After being pelleted by centrifugation at 1000 rpm (5 min), cells were washed and resuspended in PBS. Aliquots of cell suspensions were cytospun at 500 rpm for 5 min onto the superfrost Fisher brand slides and fixed in 4% paraformaldehyde for 20 min. The cells were incubated with the primary antibodies against the 4-HNE−protein adduct (1:500) prepared in blocking buffer (1% BSA and 1% goat serum in PBS) overnight at 4 °C in a humidified chamber. After being washed three times with PBS (5 min each), cells were incubated with TRITC-conjugated secondary antibodies (1:500) for 2 h at room temperature. Subsequently, this was once again followed by three washings with PBS (10 min each), and then cells were mounted with Vecta Shield containing DAPI and observed under the Nikon Eclipse E800 fluorescence microscope with a 40× objective. Different panels of photographs with DAPI and TRITC stains have been appropriately marked in the figure.

activity of γ-glutamylcysteine synthase (γ-GCS), the rate-limiting GSH-synthesizing enzyme. There was a slight but statistically insignificant increase in the GSH levels of hGSTA1-1-expressing cells. However, depletion of GSH levels upon SFN treatment was found to be comparable in the vector- and *hGSTA1*-transfected cells (data not presented), indicating that intracellular alterations in GSH levels did not contribute to the effects of *GSTA1* transfection on SFN cytotoxicity, and SFN-mediated signaling described later in this work.

Overexpression of hGSTA1-1 Inhibits SFN-Induced LPO. To assess the effect of *GSTA1* transfection on SFN-induced LPO, we compared the levels of 4-HNE in empty vector- and *hGSTA1*-transfected cells spectrophotometrically as well as by comparing the immunofluorescence using antibodies against 4-HNE. Results of these studies showed that SFN treatment caused a dose-dependent increase in cellular 4-HNE levels and that the expression of hGSTA1-1 attenuated both, the basal and SFN-induced 4-HNE levels in these cells (Figure 1C,D). Overall, our studies indicated that the overexpression of hGSTA1-1 in cells significantly suppressed the generation of 4-HNE and the accumulation of 4-HNE−protein adducts.

Table 1: Specific Activities of Antioxidant Enzymes in Empty Vector (VT)- and *hGSTA1*-Transfected HL60 Cells[a]

		specific activity [nmol min^{-1} (mg of protein)$^{-1}$; mean ± SD; n = 3]	
no.	enzyme	VT	*hGSTA1*
1	GSTs		
	CDNB[b]	66.38 ± 2.7	121.7 ± 4.6
	SFN[b]	92.0 ± 6.4	170 ± 11
2	GPx		
	CU-OOH[c]	0.175 ± 0.034	0.788 ± 0.12
3	GR	36 ± 2.4	43 ± 1.82
4	γGCS	44.4 ± 3.67	80.13 ± 4.48

[a]The activities of GSTs against 1-chloro-2,4-dinitrobenzene (CDNB) (*26*) and sulforaphane (SFN) (*27*) were measured in the crude cytosolic extracts (28000*g* supernatants) prepared from the empty vector- and *hGSTA1*-transfected cells. GPx activity against cumene hydroperoxide (CU-OOH) (*27*) and activities of GR (*28*) and γGCS (*29*) were also estimated in the crude extracts. [b]Substrates of GSTs. [c]Substrate of GPx.

Overexpression of hGSTA1-1 Attenuates SFN Cytotoxicity. To investigate the protective role of hGSTA1-1 against SFN cytotoxicity in HL60 and K562 cells, we compared the effects of SFN at different concentrations in the empty vector- and *hGSTA1*-transfected HL60 cells for a period of 24 h by an MTT assay. The IC_{50} values of SFN as determined in three independent experiments were found to be 19 ± 3.4 and 42 ± 2.6 μM for the empty vector- and hGSTA1-1-overexpressing HL60 cells, respectively, whereas the IC_{50} values of SFN for empty vector- and hGSTA1-1-overexpressing K562 cells were found to be 16.4 ± 1.64 and 39.5 ± 2.23 μM, respectively. The cell viability data presented in panels A and B of Figure 2 indicated that the expression of hGSTA1-1 in the transfected cells conferred ~2-fold resistance to SFN-induced cytotoxicity.

Overexpression of hGSTA1-1 Attenuates SFN-Induced Cell Cycle Arrest. A number of studies have shown that plant-derived isothiocyanates such as SFN exert their cytotoxicity on cancer cells through cell cycle arrest in the G2/M phase and apoptosis (*2*−*5*). These effects have been attributed to ROS-induced signaling. Since transfection with *hGSTA1* was observed to attenuate intracellular 4-HNE levels (Figure 1C), we examined if hGSTA1-1-overexpressing cells were resistant to SFN-induced cell cycle arrest. For these experiments, we treated the empty vector- and *hGSTA1*-transfected cells with 20 μM SFN for various time points and quantified the percentage of cells in the different phases of the cell cycle in the control and SFN-treated cells by flow cytometry. Microscopic observations supported by the FACS analysis data (Figure 3A−E) demonstrated that SFN (20 μM) caused a gradual time-dependent accumulation of the empty vector- and *hGSTA1*-transfected cells in the G2/M phase of the cell cycle. Vector-transfected cells, however, were significantly more susceptible to the SFN-induced cell cycle arrest in the G2/M phase and subsequent apoptosis (sub-G0/G1 cells) as compared to those expressing hGSTA1-1 (Figure 3C−E). A significant population of cells underwent apoptosis upon exposure to SFN (Figure 3B−E), and this population of apoptotic cells was significantly attenuated in *hGSTA1*-transfected cells. When empty vector- and *GSTA1*-transfected cells were allowed to recover for 24 h after SFN treatment in medium without SFN, a significantly higher percentage (~30%) of hGSTA1-1-overexpressing cells was recovered from SFN-induced G2/M cell

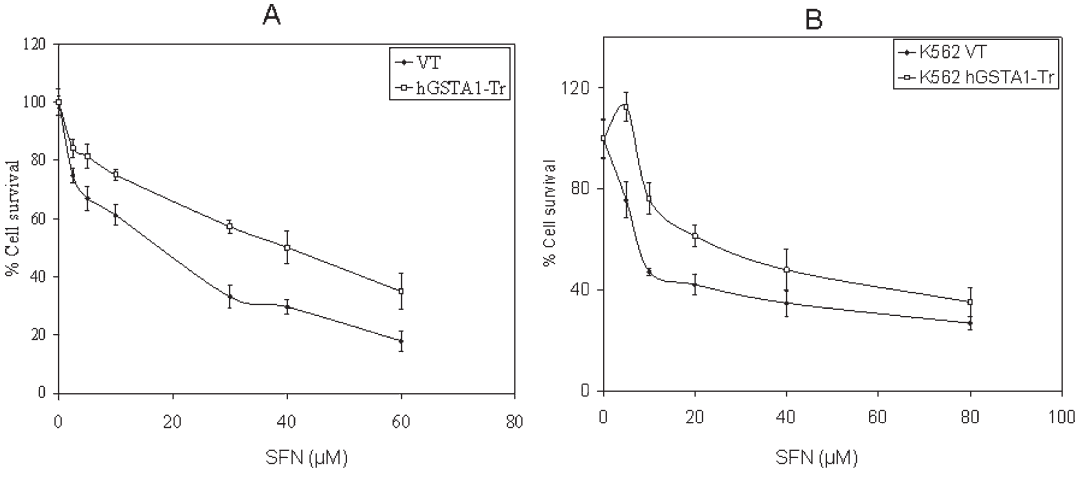

FIGURE 2: Cytotoxic effects of SFN on VT- and hGSTA1-1-expressing cells. VT- and hGSTA1-1-expressing HL60 (A) and K562 (B) cells (2×10^4) were plated into replicate wells of a 96-well plate in RPMI complete growth medium. After being incubated overnight, cells were treated with different concentrations of SFN (0−60 μM) prepared in DMSO (final concentration of 0.02%) with appropriate controls and were incubated for 24 h at 37 °C, after which the MTT assay was performed as described in Materials and Methods. The OD_{580} values of samples subtracted from those of respective blanks (no cells) were normalized with control values. The values shown are means ± SD (n = 3 done in quadruplets; $p < 0.01$).

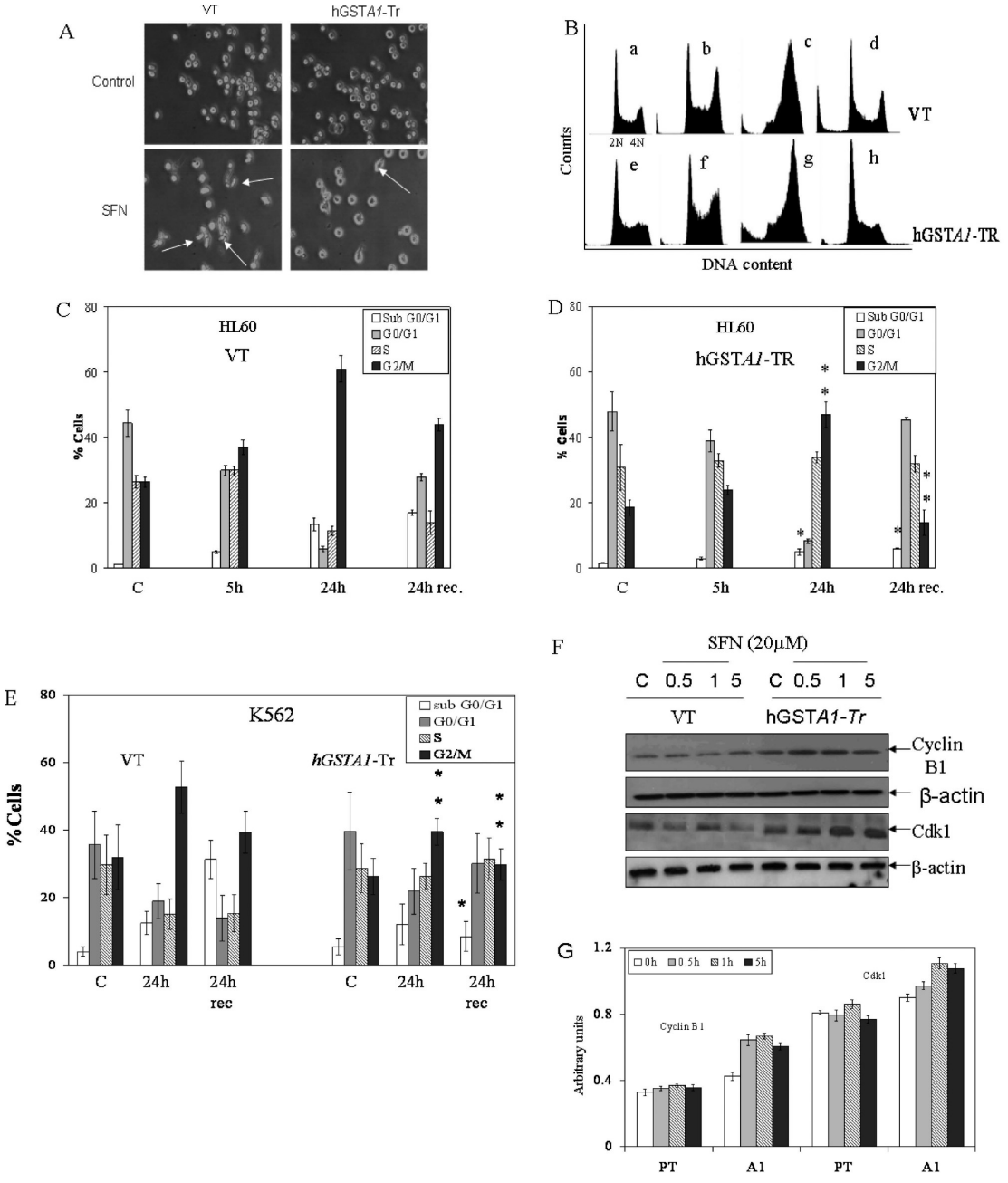

FIGURE 3: FACS analysis of the SFN-induced cell cycle arrest in VT- and hGSTA1-1-overexpressing cells. Cells (2×10^5) plated in complete growth medium were treated with SFN (20 μM) for 5 and 24 h at 37 °C with appropriate controls. Separate groups of cells were also allowed to recover for 24 h after a 24 h treatment with SFN. After the treatment, cells were pelleted, washed with PBS, and fixed in ice-cold 70% ethanol. As described in Materials and Methods, cells were stained with propidium iodide (1 mg/mL) and analyzed using the Beckman Coulter Cytomics FC500, flow cytometry analyzer. (A) Morphology of cells undergoing SFN-induced cell cycle arrest (shown by arrows) viewed under a phase contrast light microscope. (B) Flow cytometric histograms of the percentage of cells in different phases of the cell cycle [(a−d) VT-transfected cells and (e−h) *hGSTA1*-transfected cells]: (a and e) control, (b and f) 5 h SFN treatment, (c and g) 24 h SFN treatment, and (d and h) cells that had recovered for 24 h after a 24 h SFN treatment. (C and D) Bar charts showing the percentage of cells in the respective phases (sub-G0/G1, G0/G1, S, and G2/M) of the cell cycle (means ± SD) from three independent experiments. (E) Bar chart showing the effect of SFN on the cell cycle of K562 (VT- and *hGSTA1*-transfected) cells. (F) Western blot analysis of the expression of cell cycle-related proteins Cdk1 and cyclin B1, respectively, in control and SFN-treated VT- and hGSTA1-1-expressing HL60 cells. (G) Densitometric analysis of bands obtained for cyclin B1 and cdk1 on immunoblots. One asterisk and two asterisks represent significant differences in the percentages of cells in apoptosis (sub-G0/G1) and G2/M phase, respectively, in VT and hGSTA1-1.

cycle arrest as compared (~16%) to those transfected with the empty vector (Figure 3B−E). During the 24 h recovery period, the percentage of apoptotic cells in VT-transfected cells was significantly higher than the percentage of those expressing hGSTA1-1. Considering that the primary ROS detoxifying enzymes, catalase and SOD, were comparable in vector- and *hGSTA1*-transfected HL60 cells and that GSTA1-1 does not express GPx activity toward H_2O_2, these results strongly indicated that the SFN-induced accumulation of 4-HNE contributed to the cell cycle arrest of these cells and that overexpression of hGSTA1-1 rescued them from G2/M cell cycle arrest by limiting SFN-induced formation of 4-HNE.

Overexpression of hGSTA1-1 Affects Proteins Involved in SFN-Induced Cell Cycle Arrest. Cell cycle progression is

regulated by three classes of proteins, viz., cyclins, cyclin-dependent kinases (cdks), and cdk inhibitors (CKIs). During growth arrest, an increase in the levels of CKIs is reported along with a reduction in the levels of cyclins (*37*, *38*). An increase in the level of the cdk1−cyclin B1 complex is reported during the entry of cells into mitosis. Our results (Figure 3F,G) showing significantly higher levels of expression of cyclin B1 and Cdk1 (cdc2) in hGSTA1-1-overexpressing cells as compared to that in empty vector-transfected cells are consistent with the observed higher rate of recovery of GSTA1-1-overexpressing cells from SFN-induced cell cycle arrest. These results implicate the intracellular level of 4-HNE as a major determinant of cell cycle arrest and suggest that *GSTA1* transfection provides protection from SFN-induced cell cycle arrest.

Overexpression of hGSTA1-1 Affects the Apoptotic Proteins, Bcl-xL and Bax. Previous studies have shown that cells respond to various physicochemical stressors rapidly by modulating different pro- and anti-apoptotic components of the signaling machinery (*10*, *15*−*19*). Moreover, as described in the preceding section, results of FACS analysis showed that the exposure of cells to SFN induces G2/M cell cycle arrest of HL60 cells within a period of 5 h. Therefore, the effects of SFN on pro- and anti-apoptotic signaling proteins in both these cell types were analyzed after treatment for 0.5−5 h. Bcl-xL is an anti-apoptotic BH-3 only family of proteins (*39*) that is known to directly interact with the pro-apoptotic protein Bax to prevent its translocation to mitochondria, thereby inhibiting apoptosis (*40*). Results presented in Figure 4 A indicate that a significantly higher level of expression of Bcl-xL was observed in SFN-treated hGSTA1-1-overexpressing cells compared to the level of those transfected with empty vector. Our results also show (Figure 4B) the inhibition of mitochondrial translocation of Bax and the release of cytochrome *c* into cytosol (Figure 4C) in hGSTA1-1-overexpressing cells. These results are consistent with the observed resistance of GSTA1-1-overexpressing cells to SFN-induced apoptosis. Taken together, these results strongly suggest a crucial role of the LPO product, most likely 4-HNE in SFN-induced signaling for cell cycle arrest and apoptosis.

SFN-Induced Nuclear Accumulation of AIF Is Inhibited in hGSTA1-1-Overexpressing Cells. Apoptosis-inducing factor (AIF) is a bifunctional NADH oxidase involved in mitochondrial respiration and caspase-independent apoptosis (*41*, *42*). AIF plays a pro-survival role through its redox activity in mitochondria but assumes a lethal function upon being translocated to the nucleus where it causes partial chromatin condensation and DNA fragmentation (*42*). We therefore compared any possible effect of SFN on AIF in the vector- and *hGSTA1*-transfected cells. Results of these experiments (Figure 4D) showed that while in the vector-transfected cells, SFN promoted a time-dependent increase in the level of nuclear accumulation of AIF; this effect of SFN was almost completely abrogated in hGSTA1-1-overexpressing cells. Bax is reported to facilitate the nuclear accumulation of AIF (*40*). Relatively higher levels of accumulation of Bax in the mitochondria of vector-transfected cells upon SFN treatment were consistent with the observed higher levels of nuclear accumulation of AIF in these cells (Figure 4B,D). This would also be consistent with the observed higher sensitivity of the vector-transfected cells to SFN-induced apoptosis as compared to that of the hGSTA1-1-overexpressing cells. Strikingly, the lack of any significant induction of caspase-3 during SFN-induced apoptosis suggested that caspase-3-independent apoptosis in these cells may be mediated by AIF which

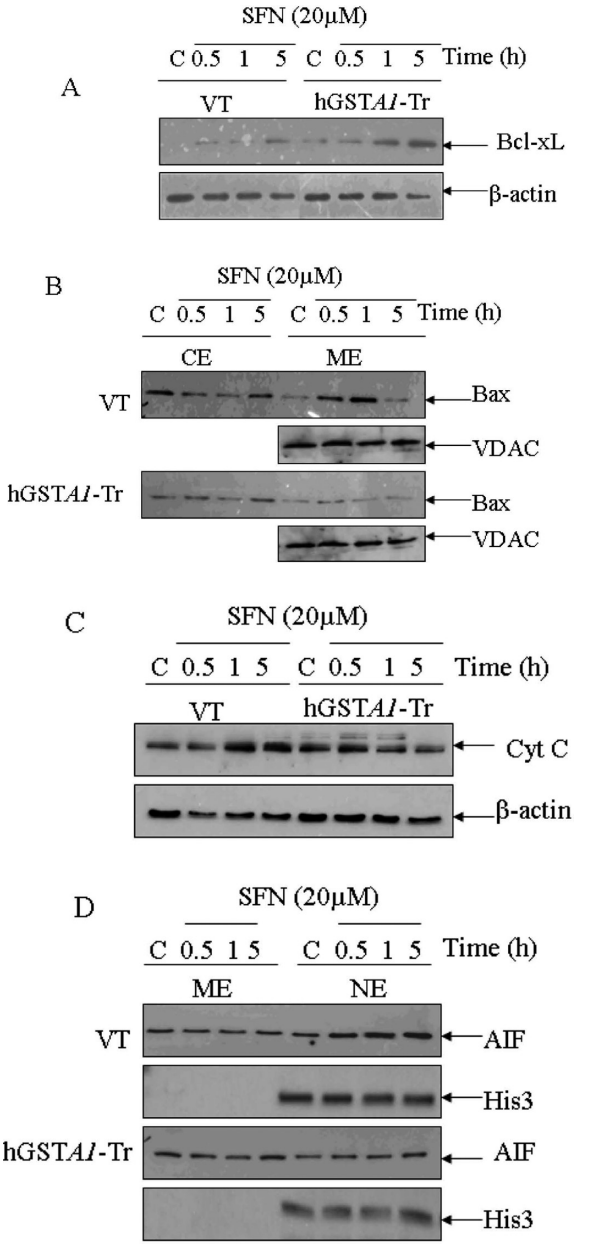

FIGURE 4: Effects of SFN on the expression of apoptosis-related proteins (Bcl-xL, Bax, AIF, and cytochrome *c*) in VT- and hGSTA1-1-expressing HL60 cells. Plated cells (5×10^6) were incubated with SFN (20 μM) in complete RPMI growth medium for different periods of time (0.5, 1, and 5 h) at 37 °C. After treatment, they were pelleted by centrifugation and washed twice with PBS. Whole cell extracts were prepared in RIPA lysis buffer while subcellular (cytoplasmic, nuclear, and mitochondrial) fractionation was performed as described in Materials and Methods and by the Imgenex Kit per the manufacturer's instructions. Western blot analyses of these extracts were conducted by using antibodies against Bcl-xL (A), Bax (B), cytochrome *c* (C), and AIF (D). Immunoblots were also probed with β-actin (total and cytoplasmic extracts) to ascertain equal loading of proteins. The blot was developed using chemiluminescence (Supersignal West Pico, Pierce) reagents to detect the bands on immunoblots.

was attenuated in *hGSTA1*-transfected cells with ameliorated 4-HNE levels.

SFN-Induced Nuclear Accumulation of Nrf2 Is Exacerbated in hGSTA1-1-Overexpressing Cells. Transcription factor Nrf2 interacts with ARE and regulates the transcription of genes encoding antioxidant proteins (*6*, *7*, *43*) involved in protection against oxidative stress. We compared the levels of

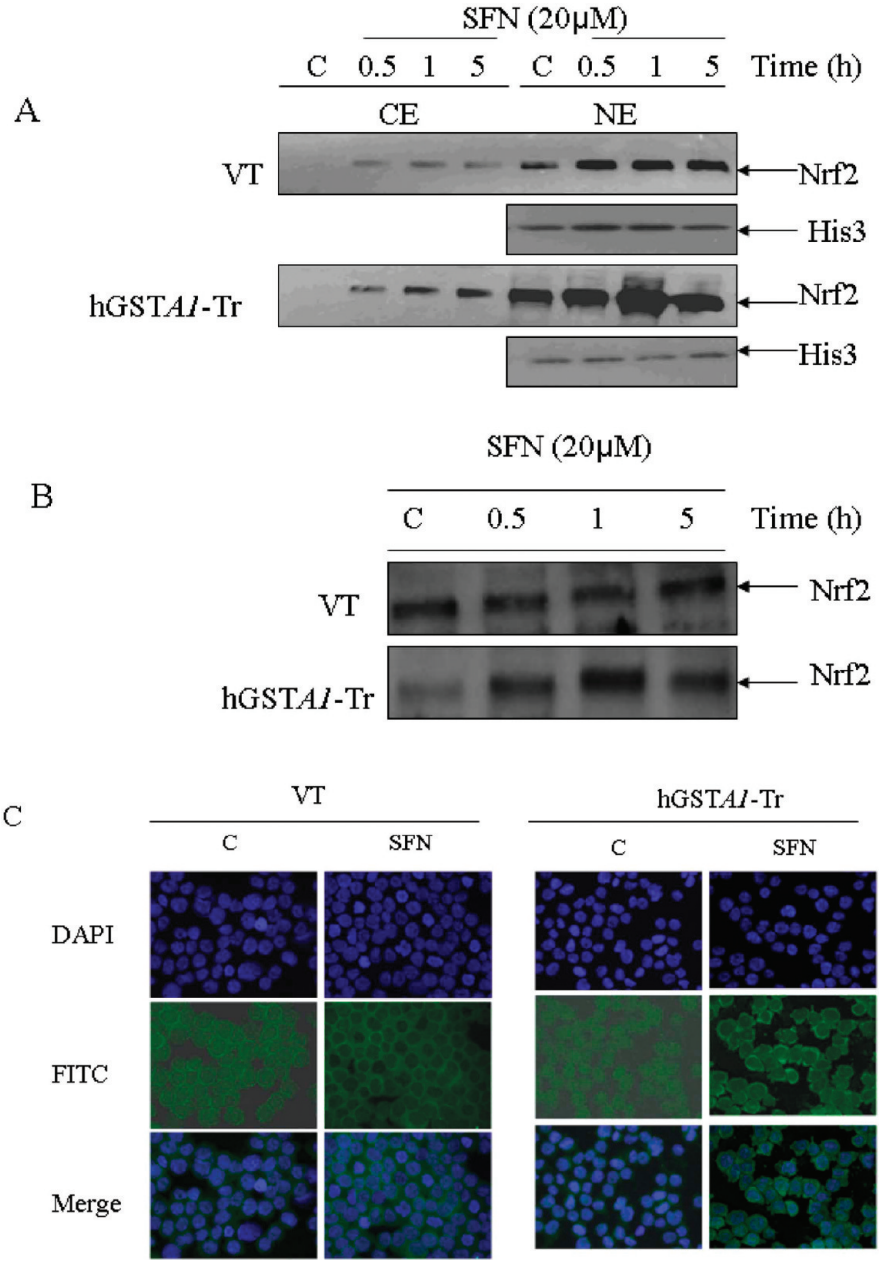

FIGURE 5: (A) Effect of SFN on the expression and localization of Nrf2 in VT- and hGSTA1-1-expressing cells. Cells were treated with SFN (20 μM) for different periods of time (0.5, 1, and 5 h). Cytoplasmic and nuclear extracts of control and treated cells were prepared and subjected to Western blot analyses as described in the legend of Figure 4. A representative Western blot showing the expression of Nrf2 in cytoplasmic and nuclear protein fractions obtained from control and SFN-treated VT- and hGSTA1-1-expressing HL60 cells. (B) Western blot of the nuclear extract of VT- and hGSTA1-1-expressing K562 cells. (C) Immunofluorescence localization of Nrf2 in control and SFN-treated VT- and hGSTA1-1-expressing HL60 cells. Control and SFN-treated cells (2×10^5) for immunolocalization of Nrf2 were essentially processed as described in the legend of Figure 2B, except that the antibodies used were those against Nrf2 (diluted 1:200 in blocking buffer) and FITC-conjugated secondary antibodies.

Nrf2 in the cytosolic and nuclear fractions of SFN-treated empty vector- and *hGSTA1*-transfected cells to study the possible role of 4-HNE in the nuclear translocation of Nrf2 upon SFN treatment. Results of these studies (Figure 5A−C) indicate that exposure to SFN led to an enhanced accumulation of Nrf2 in the nuclear extracts of both the empty vector- and *hGSTA1*-transfected cells in a time-dependent manner. Western blot analysis data (Figure 5A) indicated a rapid nuclear accumulation of Nrf2 within 30 min of SFN treatment which persisted for up to at least 5 h, thereby suggesting this to be an early event for the increased level of transcription of antioxidant enzymes to protect cells from the SFN-induced oxidative stress. The results of Western blot analysis and immunofluorescence studies clearly showed that the level of nuclear accumulation of Nrf2 was significantly higher in *hGSTA1*-transfected cells (Figure 5A−C). Nuclear translocation of Nrf2 has been suggested to be initiated by its dissociation from Keap1 during oxidative stress (*44*). Our results showing relatively higher levels of nuclear accumulation of Nrf2 in 4-HNE-depleted, hGSTA1-1-overexpressing cells suggested that SFN-induced upregulation of Nrf2 is independent of 4-HNE or lipid peroxidation and may result from the direct interaction of electrophilic SFN with the cysteine residues of Keap1.

Overexpression of hGSTA1-1 Exacerbates SFN-Induced Activation of HSF1 by Promoting Translocation of Daxx to the Cytosol. The role of transcription factor HSF1 has been suggested in the mechanisms of defense against oxidative

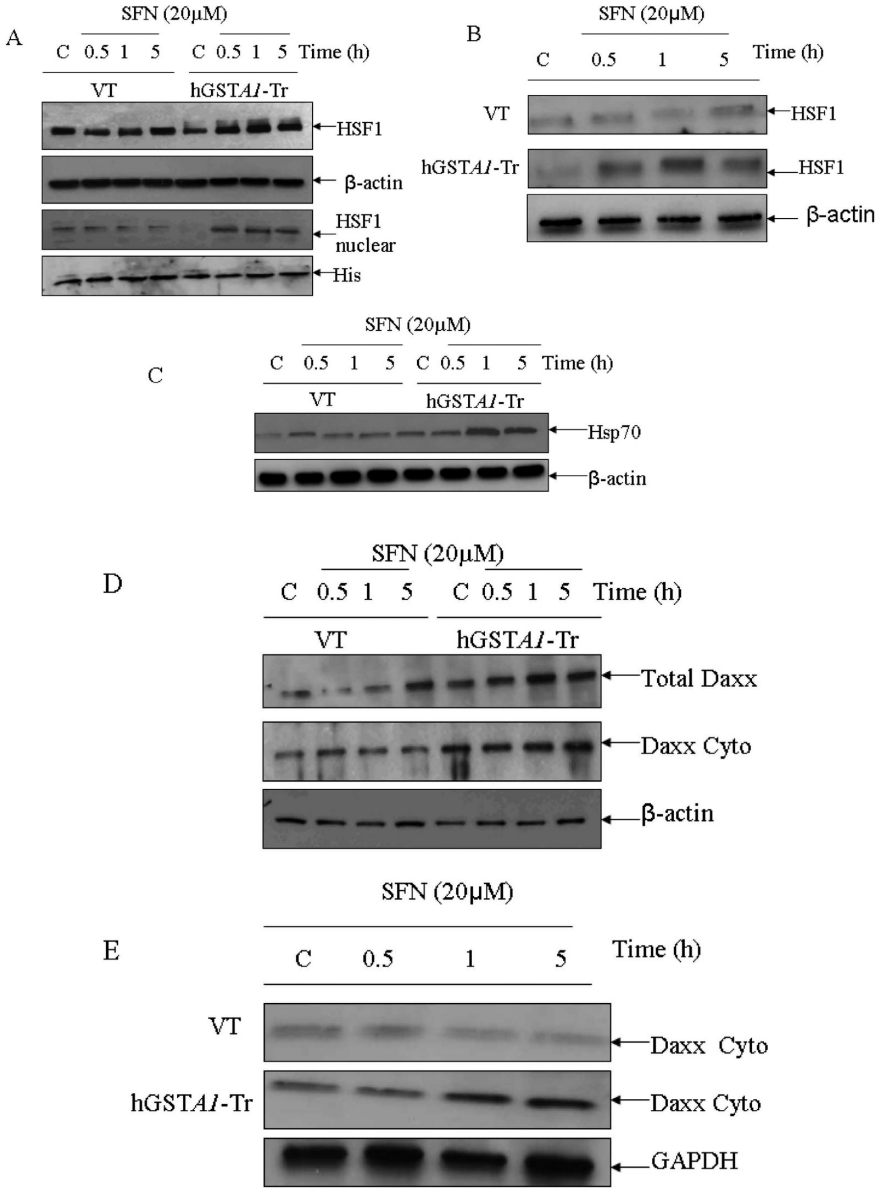

FIGURE 6: Effect of SFN on the expression and localization of HSF1 (A and B), Hsp70 (C), and Daxx (D and E) in VT- and hGSTA1-1-expressing cells. Cells (2×10^6) were treated with SFN (20 μM) in complete growth medium at 37 °C for different periods of time as shown in the figure. Total cell extracts in RIPA buffer, cytoplasmic, and nuclear fractions of the cells were prepared as described in Materials and Methods. Western blot analyses of the SDS−PAGE-resolved proteins (50−60 μg of protein in each lane) were conducted by using antibodies against Daxx, HSF1, and Hsp70 as described in Materials and Methods.

stress (*45*). Heat shock proteins (Hsps), the client proteins of HSF1, play an important role in the recovery of cells from the toxic effects of oxidative stress caused by heat, radiation, and chemicals (*19*−*21*, *45*, *46*). Western blot data presented in panels A and B of Figure 6 indicate significantly more induction and enhanced nuclear accumulation of HSF1 in SFN-treated hGSTA1-1-overexpressing HL60 and K562 cells, respectively, compared to that in vector-transfected cells. This correlated with significantly higher levels of expression of Hsp70 (Figure 6C) in the *hGSTA1*-transfected cells as compared to the vector-transfected cells.

Death-associated Fas binding protein, Daxx, has been shown to be a transcription repressor that translocates to the cytoplasm upon exposure of cells to oxidative stress (*19*, *47*). The translocation of Daxx from the nucleus to the cytoplasm has been shown to induce nuclear accumulation of HSF1 and induction of Hsp70 (*19*). Results presented in panels D and E of Figure 6 show that a time-dependent accumulation of Daxx in the cytoplasm of *hGSTA1*-transfected cells is accompanied by HSF1 activation. These effects of SFN on HSF1 and Daxx appear to be independent of 4-HNE. Taken together, our results suggest that GSTA1-1 may also protect cells from SFN-induced toxicity through the activation of stress-responsive HSF1 and Daxx.

DISCUSSION

It has already been demonstrated that exposure to SFN causes the generation of ROS in cells and tissues. Furthermore, ROS-induced cellular signaling is believed to contribute to at least some of its known chemopreventive properties (*1*−*5*). The results of our study indicate that at least some of the biological activities associated with the chemoprotective properties of SFN may be mediated through LPO products, particularly 4-HNE generated during SFN-induced oxidative stress, and that these activities can

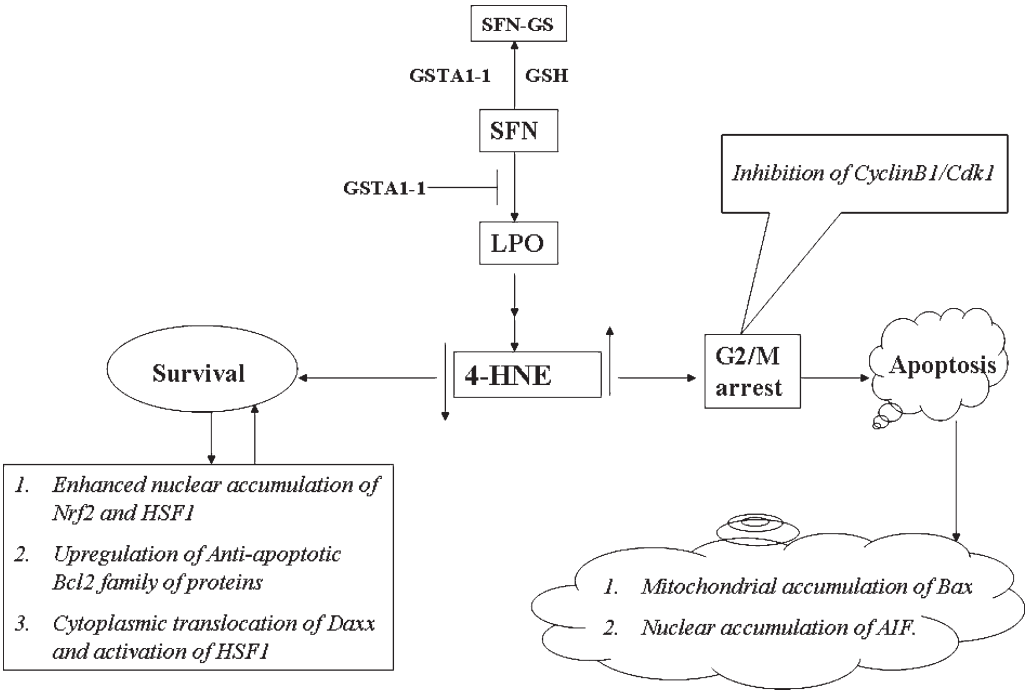

FIGURE 7: Theoretical model for the mechanisms by which SFN-induced generation and accumulation of 4-HNE affects signaling for cell cycle arrest and apoptosis and inhibition of these effects of SFN by GSTA1-1. The model illustrates that treatment of cells with SFN causes enhanced LPO-induced accumulation of 4-HNE which contributes to SFN-induced cell cycle arrest in the G2/M phase through inhibition of cyclin B1 and cdk1, and apoptosis via downregulation of anti-apoptotic Bcl-xL, an increased level of translocation of pro-apotoic Bax to mitochondria, enhanced accumulation of AIF in the nucleus, and cytoplasmic release of cytochrome *c*. These SFN-induced effects are inhibited by the enforced expression of GSTA1-1 in cells. The overexpression of GSTA1-1 limits the formation of 4-HNE by reducing upstream LPO products, which leads to the upregulation of Bcl-xL, facilitated cytoplasmic export of the transcription repressor Daxx accompanied by enhanced nuclear accumulation of transcription factors Nrf2 and HSF1, and activation of the associated stress-responsive antioxidant and heat shock proteins.

be modulated by GSTs. Overexpression of GSTA1-1 in HL60 and K562 cells was shown to suppress 4-HNE levels by limiting SFN-induced LPO and to confer a remarkable resistance to cells against SFN-mediated cytotoxicity, cell cycle arrest, and apoptosis. These findings are consistent with recent studies (*9*) showing that 4-HNE is involved in the mechanisms of ROS-mediated signaling and that GSTs play an important regulatory role in oxidative stress-induced signaling.

The attenuation of 4-HNE levels in hGSTA1-1-overexpressing cells after SFN treatment underscores the role of GSTA1-1 in regulating the levels of 4-HNE. Since 4-HNE is known to cause cell cycle arrest, apoptosis, and cytotoxicity to cells via necrosis (*48*−*50*), the observed effects of GSTA1-1 overexpression on these biological activities of SFN may be attributed to the LPO suppression capability of GSTA1-1. While it is possible that the increased SFN conjugating activity of GSTA1-1-overexpressing cells may lower the actual concentration of SFN by its accelerated conjugation with GSH, our results showing no significant alteration in the GSH levels of SFN-treated empty vector or *hGSTA1*-transfected cells suggest that the observed protective effects of GSTA1-1 against SFN toxicity may be imparted preferentially through the inhibition of SFN-induced LPO and consequent lowering of 4-HNE levels, rather than GST−GSH-mediated detoxification of SFN.

The observed effects of SFN in HL60 and K562 cells are essentially similar to those reported in previous studies with colon and prostate cancer cells (*2*, *3*). Exposure to SFN caused cell cycle arrest in the G2/M phase in both these cell types. hGSTA1-1 overexpression caused approximately 2-fold resistance to SFN-induced cell cycle arrest as well as apoptosis. Cell cycle arrest at the G2/M phase by SFN has been suggested to be regulated by cell cycle-related proteins, cyclin B1 and Cdk1, and/or disruption of normal mitotic microtubule polymerization and histone acetylation (*51*, *52*). Cyclins and cyclin-dependent kinase complexes play an important role in the G2−M transition mechanisms. By binding to Cdk1/2, cyclin B1 can activate Cdk1/2 (cdc2) to facilitate its nuclear accumulation for mitotic initiation in the late G2 phase of mammalian cells (*4*, *37*, *38*). A time-dependent induction of Cdk1 and cyclin B1 in SFN-treated hGSTA1-1-overexpressing cells indicates that the inhibition of SFN-induced accumulation of 4-HNE by hGSTA1-1 rescued them from the G2/M arrest via the upregulated expression of Cdk1 and cyclin B1. Inhibition of SFN-induced apoptosis in GSTA1-1-overexpressing cells could also be attributed to the effect of suppression of 4-HNE levels and subsequent modulation of mitochondrial apoptotic pathways. This is indicated by the activation of Bcl-xL and attenuated translocation of Bax to mitochondria in *GSTA1*-transfected cells. Furthermore, in *GSTA1*-transfected cells, the release of SFN-induced cytochrome *c* to the cytosol and nuclear accumulation of AIF are also inhibited. These findings would indicate that SFN can induce apoptosis in human erythroleukemic cells through a mitochondria-mediated caspase-independent pathway (*53*) and that this can be modulated by suppression of LPO by GSTs.

Transcriptional regulation of many genes encoding antioxidant proteins under stressful conditions for the maintenance of cellular redox homeostasis involves an important role for Nrf2, a short half-life protein, sequestered in the cytoplasm through its binding with Keap1. Nrf2 is targeted for ubiquitination when bound to its inhibitory protein Keap1 but is activated by oxidative stress when it dissociates from Keap1, translocates into the nucleus, and transactivates the antioxidant response element

(ARE) to induce the phase 2 detoxification and antioxidant enzymes (*1*, *6*−*8*). Our results of Western analysis and immunofluorescence microscopy showed nuclear accumulation of Nrf2 upon SFN exposure in the nuclei of both the empty vector- and *hGSTA1*-transfected cells. However, relatively higher levels of nuclear accumulation of Nrf2 observed in hGSTA1-1-overexpressing cells as compared to the empty vector-transfected cells may be a factor contributing to the resistance of GSTA1-1-overexpressing cells to SFN toxicity. Enhanced nuclear accumulation of Nrf2 in GSTA1-1-overexpressing cells upon treatment with SFN may also suggest a reprogramming of the protective machinery of the cells to alleviate electrophilic stress. Our results demonstrate that SFN exposure leads to nuclear translocation of HSF1 and upregulated expression of a representative HSF1 client protein, Hsp70, which correlates with the observed inhibition of SFN-induced nuclear accumulation of AIF in GSTA1-1-overexpressing cells and their resistance to apoptosis. Our results also suggest that SFN-induced upregulation of heat shock proteins most likely results from the translocation of HSF1 transcription repressor protein Daxx (*19*) from the nucleus to the cytoplasm. We demonstrate that SFN treatment promotes the translocation of Daxx from the nucleus to the cytoplasm which is accompanied by the nuclear translocation of HSF1 and upregulation of the expression of HSF1-related genes. These combined effects of GSTA1-1 should collectively contribute to the protective mechanisms against oxidative stress caused by SFN. Interestingly, these results suggest that similar to 4-HNE (*19*), SFN also induces mechanisms to self-limit its own toxicity. Since GSTA1-1-overexpressing cells with subconstitutive 4-HNE levels show a higher degree of activation of Nrf2 and HSF1, it appears unlikely that 4-HNE is involved in upregulation of these parameters. Instead, SFN, being a strong electrophilic compound, can directly interact with Keap1 and Daxx to affect the activation of Nrf2 and HSF1, respectively.

In summary, the results of our studies indicate that SFN-induced LPO contributes to its cytotoxicity to cells which can be inhibited by the overexpression of GSTA1-1 and that the protective effects of GSTA1-1 are associated with its ability to regulate 4-HNE levels in cells. GSTA1-1 and possibly other α-class GSTs seem to play a crucial role in protecting cells from the cell cycle arrest and apoptotic effects of SFN through a well-orchestrated interplay of several pro-survival signaling pathways as presented in a model shown in Figure 7. Perhaps this model can be extrapolated to the overall protective role of GSTs during oxidative/electrophilic stress and the role of 4-HNE in the regulation of signaling. Further studies are needed to validate this model, particularly for deciphering the mechanisms of interplay between Nrf2 and HSF1 and associated genes upon exposure to agents that promote LPO.

ACKNOWLEDGMENT

We thank Xiangle Sun (Core Facility at the University of North Texas Health Science Center) for helping with flow cytometry and laser capture microdissection (supported by National Institutes of Health Grant ISIORR018999-01A1).

REFERENCES

1. Juge, N., Mithen, R. F., and Traka, M. (2007) Molecular basis for chemoprevention by sulforaphane: A comprehensive review. *Cell. Mol. Life Sci. 64*, 1105–1127.
2. Payrastre, G. L., Li, P., Lumeau, S., Cassar, G., Dupont, M. A., Chevolleau, S., Gasc, N., Tulliez, J., and Tercé, F. (2000) Sulforaphane, a naturally occurring isothiocyanate, induces cell cycle arrest and apoptosis in HT29 human colon cancer cells. *Cancer Res. 60*, 1426–1433.
3. Singh, S. V., Herman-Antosiewicz, A., Singh., A. V., Lew, K. L., Srivastava, S. K., Kamath, R., Brown, K. D., Zhang, L., and Baskaran, R. (2004) Sulforaphane-induced G2/M phase cell cycle arrest involves checkpoint kinase 2-mediated phosphorylation of cell division cycle 25C. *J. Biol. Chem. 279*, 25813–25822.
4. Singh, S. V., Srivastava, S. K., Choi, S., Lew, K. L., Antosiewicz, J., Xiao, D., Zeng, Y., Watkins, S. C., Johnson, C. S., Trump, D. L., Lee, Y. J., Xiao, H., and Herman-Antosiewicz, A. (2005) Sulforaphane-induced cell death in human prostate cancer cells is initiated by reactive oxygen species. *J. Biol. Chem. 280*, 19911–19924.
5. Xiao, D., Srivastava, S. K., Lew, K. L., Zeng, Y., Hershberger, P., Johnson, C. S., Trump, D. L., and Singh, S. V. (2003) Allyl isothiocyanate, a constituent of cruciferous vegetables, inhibits proliferation of human prostate cancer cells by causing G2/M arrest and inducing apoptosis. *Carcinogenesis 24*, 891–897.
6. McWalter, G. K., Higgins, L. G., McLellan, L. I., Henderson, C. J., Song, L., Thornalley, P. J., Itoh, K., Yamamoto, M., and Hayes, J. D. (2004) Transcription factor Nrf2 is essential for induction of NAD(P)H:quinone oxidoreductase 1, glutathione S-transferases, and glutamate cysteine ligase by broccoli seeds and isothiocyanates. *J. Nutr. 134*, 3499S–3506S.
7. Zhang, Y. (2004) Cancer-preventive isothiocyanates: Measurement of human exposure and mechanism of action. *Mutat. Res. 555*, 173–190.
8. Thimmulappa, R. K., Mai, K. H., Srisuma, S., Kensler, T. W., Yamamoto, M., and Biswal, S. (2002) Identification of Nrf2-regulated genes induced by the chemopreventive agent sulforaphane by oligonucleotide microarray. *Cancer Res. 62*, 5196–5203.
9. Yang, Y., Sharma, R., Sharma, A., Awasthi, S., and Awasthi, Y. C. (2003) Lipid peroxidation and cell cycle signaling: 4-Hydroxynonenal, a key molecule in stress mediated signaling. *Acta Biochim. Pol. 50*, 319–336.
10. Cheng, J. Z., Singhal, S. S., Sharma, A., Saini, M., Yang, Y., Awasthi, S., Zimniak, P., and Awasthi, Y. C. (2001) Transfection of mGSTA4 in HL-60 cells protects against 4-hydroxynonenal-induced apoptosis by inhibiting JNK-mediated signaling. *Arch. Biochem. Biophys. 392*, 197–207.
11. Cheng, J. Z., Singhal, S. S., Saini, M., Singhal, J., Piper, J. T., Van Kuijk, F. J., Zimniak, P., Awasthi, Y. C., and Awasthi, S. (1999) Effects of mGST A4 transfection on 4-hydroxynonenal-mediated apoptosis and differentiation of K562 human erythroleukemia cells. *Arch. Biochem. Biophys. 372*, 29–36.
12. Sharma, R., Brown, D., Awasthi, S., Yang, Y., Sharma, A., Patrick, B., Saini, M. K., Singh, S. P., Zimniak, P., Singh, S. V., and Awasthi, Y. C. (2004) Transfection with 4-hydroxynonenal-metabolizing glutathione S-transferase isozymes leads to phenotypic transformation and immortalization of adherent cells. *Eur. J. Biochem. 271*, 1690–1701.
13. Awasthi, Y. C., Sharma, R., Sharma, A., Yadav, S., Singhal, S. S., Chaudhary, P., and Awasthi, S. (2008) Self-regulatory role of 4-hydroxynonenal in signaling for stress-induced programmed cell death. *Free Radical Biol. Med. 45*, 111–118.
14. Yang, Y., Sharma, R., Cheng, J. Z., Saini, M. K., Ansari, N. H., Andley, U. P., Awasthi, S., and Awasthi, Y. C. (2002) Protection of HLE B-3 cells against hydrogen peroxide- and naphthalene-induced lipid peroxidation and apoptosis by transfection with hGSTA1 and hGSTA2. *Invest. Ophthalmol. Visual Sci. 43*, 434–445.
15. Yang, Y., Cheng, J. Z., Singhal, S. S., Saini, M., Pandya, U., Awasthi, S., and Awasthi, Y. C. (2001) Role of glutathione S-transferases in protection against lipid peroxidation: Overexpression of hGSTA2-2 in K562 cells protects against hydrogen peroxide induced apoptosis and inhibits JNK and caspase 3 activation. *J. Biol. Chem. 276*, 19220–19230.
16. Yang, Y., Sharma, A., Sharma, R., Patrick, B., Singhal, S. S., Zimniak, P., Awasthi, S., and Awasthi, Y. C. (2003) Cells preconditioned with mild, transient UVA irradiation acquire resistance to oxidative stress and UVA-induced apoptosis: Role of 4-hydroxynonenal in UVA-mediated signaling for apoptosis. *J. Biol. Chem. 278*, 41380–41388.
17. Sharma, A., Patrick, B., Li, J., Sharma, R., Jeyabal, P. V. S., Reddy, P. M. R. V., Awasthi, S., and Awasthi, Y. C. (2006) Glutathione S-transferases as antioxidant enzymes: Small cell lung cancer (H69) cells transfected with *hGSTA1* resist doxorubicin-induced apoptosis. *Arch. Biochem. Biophys. 452*, 165–173.
18. Li, J., Sharma, R., Patrick, B., Sharma, A., Jeyabal, P. V., Reddy, P. M., Saini, M. K., Dwivedi, S., Dhanani, S., Ansari, N. H., Zimniak, P., Awasthi, S., and Awasthi, Y. C. (2006) Regulation of CD95 (Fas)

expression and Fas-mediated apoptotic signaling in HLE B-3 cells by 4-hydroxynonenal. *Biochemistry 45*, 12253–12264.
19. Sharma, R., Sharma, A., Dwivedi, S., Zimniak, P., Awasthi, S., and Awasthi, Y. C. (2008) 4-Hydroxynonenal self-limits Fas-mediated DISC-independent apoptosis by promoting export of Daxx from the nucleus to the cytosol and its binding to Fas. *Biochemistry 47*, 143–156.
20. Chen, Z. H., Saito, Y., Yoshida, Y., Sekine, A., Noguchi, N., and Niki, E. (2005) 4-Hydroxynonenal induces adaptive response and enhances PC12 cell tolerance primarily through induction of thioredoxin reductase 1 via activation of Nrf2. *J. Biol. Chem. 280*, 41921–41927.
21. Jacobs, A. T., and Marnett, L. J. (2009) HSF1-mediated BAG3 expression attenuates apoptosis in 4-hydroxynonenal-treated colon cancer cells via stabilization of anti-apoptotic Bcl-2 proteins. *J. Biol. Chem. 284*, 9176–9183.
22. Jacobs, A. T., and Marnett, L. J. (2007) Heat shock factor 1 attenuates 4-hydroxynonenal-mediated apoptosis: Critical role for heat shock protein 70 induction and stabilization of Bcl-xL. *J. Biol. Chem. 282*, 33412–33420.
23. Zhao, T., Singhal, S. S., Piper, J. T., Cheng, J., Pandya, U., Clark-Wronski, J., Awasthi, S., and Awasthi, Y. C. (1999) The role of human glutathione S-transferases hGSTA1-1 and hGSTA2-2 in protection against oxidative stress. *Arch. Biochem. Biophys. 367*, 216–224.
24. Koeffler, H. P., and Golde, D. W. (1980) Human myeloid leukemic cell lines: A review. *Blood 56*, 344–350.
25. Singhal, S. S., Saxena, M., Ahmad, H., Awasthi, S., Haque, A. K., and Awasthi, Y. C. (1992) Glutathione S-transferases of human lung: Characterization and evaluation of the protective role of the α-class isozymes against lipid peroxidation. *Arch. Biochem. Biophys. 299*, 232–241.
26. Habig, W. H., Pabst, M. J., and Jakoby, W. B. (1974) Glutathione S-transferases. The first enzymatic step in mercapturic acid formation. *J. Biol. Chem. 249*, 7130–7139.
27. Kolm, R. H., Danielson, U. H., Zhang, Y., Talalay, P., and Mannervik, B. (1995) Isothiocyanates as substrates for human glutathione transferases: Structure-activity studies. *Biochem. J. 311*, 453–459.
28. Awasthi, Y. C., Beutler, E., and Srivastava, S. K. (1975) Purification and properties of human erythrocyte glutathione peroxidase. *J. Biol. Chem. 250*, 5144–5149.
29. Carlberg, I., and Mannervik, B. (1985) Glutathione reductase. *Methods Enzymol. 113*, 484–490.
30. Seelig, G. F., and Meister, A. (1984) γ-Glutamylcysteine synthetase. Interactions of an essential sulfhydryl group. *J. Biol. Chem. 259*, 3534–3538.
31. Bradford, M. M. (1976) A rapid and sensitive method for the quantitation of microgram quantities of protein utilizing the principle of protein-dye binding. *Anal. Biochem. 72*, 248–254.
32. Laemmli, U. K. (1970) Cleavage of structural proteins during the assembly of the head of bacteriophage T4. *Nature 227*, 680–685.
33. Towbin, H., Staehelin, T., and Gordon, J. (1979) Electrophoretic transfer of proteins from polyacrylamide gels to nitrocellulose sheets: Procedure and some applications. *Proc. Natl. Acad. Sci. U.S.A. 76*, 4350–4354.
34. Englander, E. W., Hu, Z., Sharma, A., Lee, H. M., Wu, Z. H., and Greeley, G. H. (2002) Rat MYH, a glycosylase for repair of oxidatively damaged DNA, has brain-specific isoforms that localize to neuronal mitochondria. *J. Neurochem. 83*, 1471–1480.
35. Mosmann, T. (1983) Rapid colorimetric assay for cellular growth and survival: Application to proliferation and cytotoxicity assays. *J. Immunol. Methods 65*, 55–63.
36. Beutler, E. (1984) Red Cell Metabolism. In A Manual of Biochemical Methods, Grune and Stratton, Orlando, FL.
37. Takizawa, C. G., and Morgan, D. O. (2000) Control of mitosis by changes in the subcellular location of cyclin-B1-Cdk1 and Cdc25C. *Curr. Opin. Cell Biol. 12*, 658–665.
38. Sánchez, I., and Dynlacht, B. D. (2005) New insights into cyclins, CDKs, and cell cycle control. *Semin. Cell Dev. Biol. 16*, 311–321.
39. Kaufmann, T., Schinzel, A., and Borner, C. (2004) Bcl-w(edding) with mitochondria. *Trends Cell Biol. 14*, 8–12.
40. Ganju, N., and Eastman, A. (2002) Bcl-X(L) and calyculin A prevent translocation of Bax to mitochondria during apoptosis. *Biochem. Biophys. Res. Commun. 291*, 1258–1264.
41. Candé, C., Cohen, I., Daugas, E., Ravagnan, L., Larochette, N., Zamzami, N., and Kroemer, G. (2002) Apoptosis-inducing factor (AIF): A novel caspase-independent death effector released from mitochondria. *Biochimie 84*, 215–222.
42. Lorenzo, H. K., Susin, S. A., Penninger, J., and Kroemer, G. (1999) Apoptosis inducing factor (AIF): A phylogenetically old, caspase-independent effector of cell death. *Cell Death Differ. 6*, 516–524.
43. Kwak, M. K., Itoh, K., Yamamoto, M., Sutter, T. R., and Kensler, T. W. (2001) Role of transcription factor Nrf2 in the induction of hepatic phase 2 and antioxidative enzymes in vivo by the cancer chemoprotective agent, 3H-1,2-dimethiole-3-thione. *Mol. Med. 7*, 135–145.
44. Dinkova-Kostova, A. T., Holtzclaw, W. D., Cole, R. N., Itoh, K., Wakabayashi, N., Katoh, Y., Yamamoto, M., and Talalay, P. (2002) Direct evidence that sulfhydryl groups of Keap1 are the sensors regulating induction of phase 2 enzymes that protect against carcinogens and oxidants. *Proc. Natl. Acad. Sci. U.S.A. 99*, 11908–11913.
45. Dai, C., Whitesell, L., Rogers, A. B., and Lindquist, S. (2007) Heat shock factor 1 is a powerful multifaceted modifier of carcinogenesis. *Cell 130*, 1005–1118.
46. Nollen, E. A., and Morimoto, R. I. (2002) Chaperoning signaling pathways: Molecular chaperones as stress-sensing 'heat shock' proteins. *J. Cell Sci. 115*, 2809–2816.
47. Salomoni, P., and Khelifi, A. F. (2006) Daxx: Death or survival protein? *Trends Cell Biol. 16*, 97–104.
48. Esterbauer, H., Schaur, R. J., and Zollner, H. (1991) Chemistry and biochemistry of 4-hydroxynonenal, malonaldehyde and related aldehydes. *Free Radical Biol. Med. 11*, 81–128.
49. Barrera, G., Pizzimenti, S., Muraca, R., Barbiero, G., Bonelli, G., Baccino, F. M., Fazio, V. M., and Dianzani, M. U. (1996) Effect of 4-hydroxynonenal on cell cycle progression and expression of differentiation-associated antigens in HL-60 cells. *Free Radical Biol. Med. 20*, 455–462.
50. Awasthi, Y. C., Sharma, R., Cheng, J. Z., Yang, Y., Sharma, A., Singhal, S. S., and Awasthi, S. (2003) Role of 4-hydroxynonenal in stress-mediated apoptosis signaling. *Mol. Aspects Med. 24*, 219–230.
51. Jackson, S. J. T., and Singletary, K. W. (2004) Sulforaphane inhibits human MCF-7 mammary cancer cell mitotic progression and tubulin polymerization. *J. Nutr. 134*, 2229–2236.
52. Dashwood, R. H., and Ho, E. (2007) Dietary histone deacetylase inhibitors: From cells to mice to man. *Semin. Cancer Biol. 17*, 363–369.
53. Joza, N., Susin, S. A., Daugas, E., Stanford, W. L., Cho, S. K., Li, C. Y., Sasaki, T., Elia, A. J., Cheng, H. Y., Ravagnan, L., Ferri, K. F., Zamzami, N., Wakeham, A., Hakem, R., Yoshida, H., Kong, Y. Y., Mak, T. W., Zúñiga-Pflücker, J. C., Kroemer, G., and Penninger, J. M. (2001) Essential role of the mitochondrial apoptosis-inducing factor in programmed cell death. *Nature 410*, 549–554.